The Measurement of Natural Alpha-Particles Ejected from Solids

ROBLEY D. EVANS,* *Physics Department, University of California, Berkeley, California*
(Received August 24, 1933)

Exact expressions for the ionization due to the emission of alpha-particles from radioactive solids are set up and the results of their graphical integration are given. The total ionization per cm² of surface, both with and without absorbers; the variation of ionization with height above the radioactive surface; the ionization from thin films; the ionization from substances containing all members of the U, Th and Ac series, both with and without absorbers; and the counting rate for alpha-particle counting chambers, are given in equations accompanied by appropriate graphs and tables. The older approximate theories break down for actual alpha-particles, particularly those of short range. If q is ion pairs per cm² per sec. formed above the surface of a radioactive solid; N, the number of alpha-particles per sec. per cm³ emitted in the solid; k, ion pairs per alpha-particle of range R in air; and R', the alpha-particle range in the solid: then $q=\epsilon NkR'$, and the numerical coefficient ϵ has values between 0.114 and 0.150 for the alpha-particles from all known radioactive substances.

I. INTRODUCTION

TWENTY years ago McCoy,[1] v. Schweidler,[2] and Flamm[3] gave an approximate theory of the ionization above a solid radioactive body, due to its emission of alpha-particles. Their work was based on the assumption that the ionization produced by an alpha-particle of range R is $k_0R^{\frac{3}{2}}$, where k_0 is a constant. Although this expression is quite accurate for all the alpha-particles of the U, Th and Ac series, where $R>2.5$ cm of air, it breaks down seriously for shorter range alpha-particles, such as are being investigated by v. Hevesy, Pahl and Hosemann,[4] Latimer and Libby,[5] Langer and Raitt,[6] and Evans and Henderson[7] and it also fails for the short residual ends of originally long range alpha-particles emerging from solids such as ordinary rocks.[8] By combining the reliable empirical ionization curves for alpha-particles obtained by G. H. Henderson[9] and others,[10] with a new mode of analytical attack, an exact solution of the problems can now be given.

II. COMPARISON OF APPROXIMATE AND ACTUAL ALPHA-PARTICLE IONIZATION CURVES

If R is the range of an alpha-particle in air at 0°C and 760 mm Hg, and r is the distance, also expressed in cm of standard air, from the origin of the track to a point under consideration, then provided $R-r\geq 2.5$ cm, we have the approximate empirical law that the number of ion pairs, I,

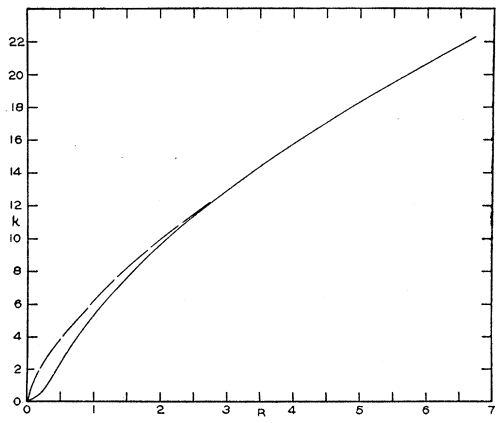

FIG. 1. The solid curve shows the empirical total ionization, k, per alpha-particle in ion pairs $\times 10^{-4}$, obtained by graphical integration over curve I of Fig. 4. The dotted curve shows the approximate value of the total ionization as given by the two-thirds power rule of Eq. (1). R is the range of the alpha-particle in cm of air at 0°C and 760 mm Hg.

* National Research Fellow.

[1] McCoy, Phys. Rev. **1**, 393 (1913).

[2] v. Schweidler, Phys. Zeits. **14**, 505, 728 (1913).

[3] Flamm, Phys. Zeits. **14**, 812, 1122 (1913).

[4] v. Hevesy, Pahl and Hosemann, Zeits. f. Physik **83**, 43 (1933).

[5] Latimer and Libby, J. Am. Chem. Soc. **55**, 433 (1933).

[6] Langer and Raitt, Phys. Rev. **43**, 585 (1933).

[7] Evans and Henderson, Phys. Rev. **44**, 59 (1933).

[8] Evans, Phys. Rev. **45**, 38 (1934).

[9] G. H. Henderson, Phil. Mag. **42**, 538 (1921).

[10] H. Geiger, Zeits. f. Physik **8**, 45 (1921); I. Curie and Behounek, J. de Physique **7**, 125 (1926); G. H. Briggs, Proc. Roy. Soc. **A114**, 341 (1927).

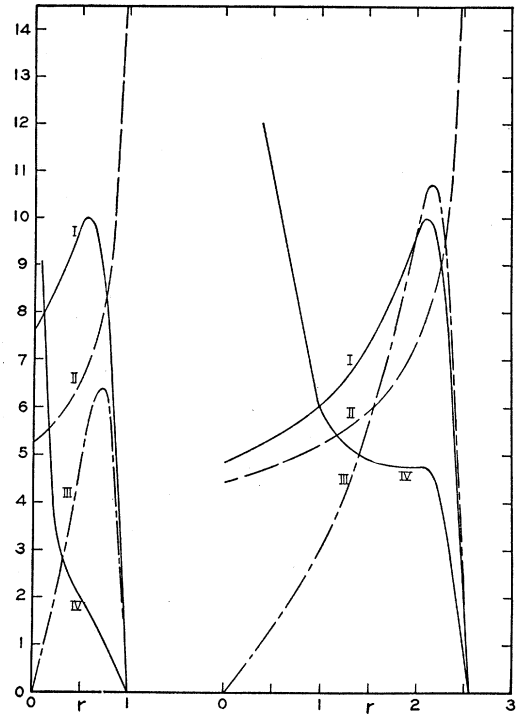

FIG. 2

FIG. 3

FIG. 2. The characteristic curves for a 1.0 cm alpha-particle in air at 0°C and 760 mm Hg. Curve I shows $\varphi(r)$, the Henderson empirical ionization per cm. Curve II shows $\Phi(r)$, the ionization per cm derived from the two-thirds power rule of Eq. (3). Curve III shows the function $r\,\varphi(r)$ and curve IV the function $1/r\,\varphi(r)$ of Eq. (6). The ordinates, on the same scale for all curves, are arbitrary. Abscissas are in cm at 0°C and 760 mm Hg.

FIG. 3. The characteristic curves for the 2.56 cm alpha-particles from U I. As in Fig. 2, curve I is $\varphi(r)$, curve II is $\Phi(r)$, curve III is $r\,\varphi(r)$, curve IV is $(1/r)\varphi(r)$. The numerical value of the ordinates for curve III are twice those shown on the scale. The areas under curves I and II are equal. Abscissas are in cm at 0°C and 760 mm Hg.

produced between r and the end of the track is

$$I=k_0(R-r)^{\frac{2}{3}} \tag{1}$$

where k_0 is a constant. The ionization per unit length of path, $\Phi(r)$, at any r is therefore

$$\Phi(r)=-\partial I/\partial r=(2/3)k_0(R-r)^{-\frac{1}{3}} \tag{2}$$

and if K is the number of ion pairs produced along the entire track from $r=0$ to $r=R$, then $K=k_0R^{\frac{2}{3}}$, and

$$\Phi(r)=(2/3)KR^{-\frac{2}{3}}(R-r)^{-\frac{1}{3}}. \tag{3}$$

This approximate expression has been used by Siegl[11] and others; it will be compared with the experimental ionization-density, $\varphi(r)$, *vs.* r curves. In the computations described below, Henderson's ionization-density *vs.* r curve for Ra C′ has been taken as accurately representing the number of ion pairs per cm, $\varphi(r)$, produced at any distance $R-r$ from the end of any alpha-particle track. The total ionization due to short range alpha-particles is obtained by graphical integration of the end portion of this $\varphi(r)$ *vs.* r curve.

Fig. 1 compares this empirical total ionization, k, with the approximate values, K, computed from the equation $K=k_0R^{\frac{2}{3}}$, k_0 being chosen to make the curves coincide at $R=6.59$ cm, Henderson's value for Ra C′ alpha-particles at 0°C and 760 mm Hg. The approximate and empirical curves agree for $R>2.56$ cm, the shortest (uranium-I) alpha-particle in the U, Th or Ac series, but K is 16 percent high for $R=1$ cm (samarium[4]), and 100 percent high for $R=0.4$ cm.

Figs. 2, 3, 4 illustrate the contrast between the empirical ionization-density curve, $\varphi(r)$, and the approximate analytic expression $\Phi(r)$, for alpha-particles of 1 cm (Sm, Be?), 2.56 cm (U I), and

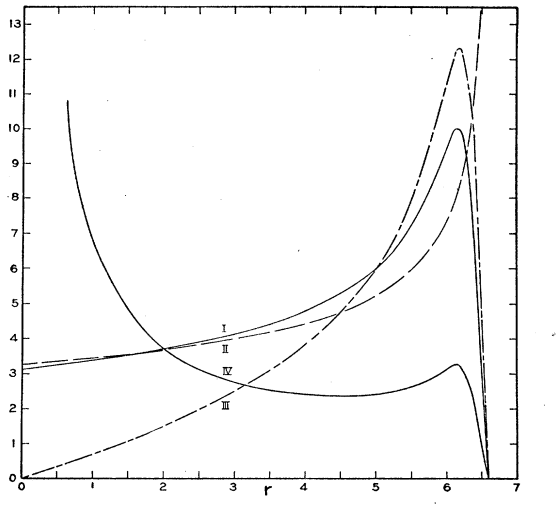

FIG. 4. The characteristic curves for the 6.60 cm alpha-particles from Ra C′. Curve I is Henderson's[9] empirical ionization curve. As in Fig. 2, curve I is $\varphi(r)$, curve II is $\Phi(r)$, curve III is $r\varphi(r)$, curve IV is $(1/r)\varphi(r)$. The ordinates are arbitrary for curve I; for curve II read ordinates as shown; for curve III multiply ordinates by 5; for curve IV multiply ordinates by 0.5. The area under curves I and II are equal. Abscissas are in cm at 0°C and 760 mm Hg.

[11] Siegl, Akad. Wiss. Wien, Ber. IIa **134**, 11 (1925).

6.59 cm (Ra C′) range. The ordinates are adjusted so that the areas under the $\varphi(r)$ and $\Phi(r)$ curves are identical, i.e., $K=k$. It is evident that agreement between $\varphi(r)$ and $\Phi(r)$ is not even remote, except in the Ra C′ curve for $r \leq 0.6\ R$.

III. Total Ionization above a Thick Solid Emitting Alpha-Particles

As here used, a thick plate is one whose thickness is greater than the range, R', of the alpha-particle in the solid, while a thin plate has a thickness less than R'. In Fig. 5, let AA' be the

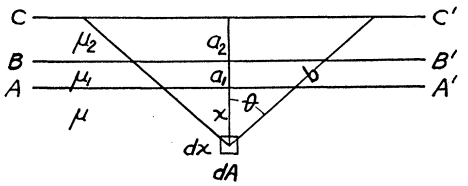

FIG. 5. Geometry for Eqs. (6), (9) and (10).

interface between a thick solid body of infinite extent emitting N alpha-particles per cm³ per sec., and an absorber of thickness a_1, above it. Similarly, let BB' be the interface between this first absorber and a second absorber of thickness a_2, and let CC' be the boundary between the second absorber and an ionization chamber. Let the stopping power of the air relative to the solid, i.e., the ratio of the alpha-particle range in the solid to its range in air, be μ for the radioactive source, μ_1 for the first absorber, μ_2 for the second absorber.

From geometry, the number of alpha-particles from a volume element $dx\,dA$ which spend the portion of their range between r and $r+dr$ above the interface CC', is the number of alpha-particles formed in the volume element $dx\,dA$, times the solid angle for emergence, or

$$[N\,dx\,dA]\left[\frac{1}{2}\left(1-\frac{x+a_1+a_2}{b}\right)\right],$$

where b is the geometrical length corresponding to a path equivalent to r cm of air. Thus $b\cos\vartheta = x+a_1+a_2$, while $r\cos\vartheta = x/\mu+a_1/\mu_1+a_2/\mu_2$, and hence $b=r(x+a_1+a_2)/(x/\mu+a_1/\mu_1+a_2/\mu_2)$. The total number, n_a, of alpha-particles per cm² of surface with the range-element between r and $r+dr$ above the interface CC', is:

$$n_a=\frac{N}{2}\int_0^{\mu(r-a_1/\mu_1-a_2/\mu_2)} 1-\frac{(x/\mu+a_1/\mu_1+a_2/\mu_2)}{r}dx \quad (4)$$

$$=\frac{N}{4}\mu(r-a)^2/r, \text{ where } a\equiv a_1/\mu_1+a_2/\mu_2+\cdots, \quad (5)$$

a being the total absorber thickness, measured in equivalent cm of air. Since the stopping power varies slightly[12] with the velocity of the alpha-particle the values of μ, μ_1, μ_2, $\cdots$ chosen for numerical work may be taken as the mean values for the range under consideration. Eq. (5) is easily generalized for any number of absorbers.

The ionization, q_a, in ion pairs per cm² per sec. due to these emergent alpha-particles is

$$q_a=\int_a^R n_a\varphi(r)dr$$

$$=\frac{N}{4}\mu\left\{\int_a^R r\varphi(r)dr-2a\int_a^R\varphi(r)dr+a^2\int_a^R\frac{1}{r}\varphi(r)dr\right\} \quad (6)$$

$$\equiv\epsilon_a kRN\mu, \quad (7)$$

where the dimensionless numerical coefficient ϵ_a is defined by Eqs. (6) and (7).

Graphical integration of Eq. (6) shows that ϵ_a depends upon R in the manner shown in Figs. 6 and 7. With no absorption (i.e., $a=0$; $\epsilon_a\equiv\epsilon$) Fig. 6 shows that ϵ is always less than 0.150, and falls to low values for short range alpha-particles. The ratio ϵ_a/ϵ, or q_a/q, is the fraction of the total ionization appearing above an absorber having a stopping power equal to a cm of air. This ratio is also a function of R and is shown in Fig. 7.

[12] Harper and Salaman, Proc. Roy. Soc. **A127**, 175 (1930).

In the limiting case of a very long range alpha-particle Eqs. (1) and (3), describing the two-thirds power rule, give nearly the same result as the exact theory. Substituting $\Phi(r)$ from Eq. (3) for $\varphi(r)$ in Eq. (6), and integrating, we obtain

$$q_a=\frac{3}{20}NKR\left\{\left(1-\frac{a}{R}\right)^{\frac{5}{3}}-\frac{5}{3}\frac{a}{R}\left(1-\frac{a}{R}\right)^{\frac{2}{3}}+\frac{5}{9}\frac{a^2}{R^2}\log\frac{1+(1-a/R)^{\frac{1}{3}}+(1-a/R)^{\frac{2}{3}}}{a^2/R^2}\right.$$
$$\left.-\frac{10}{9}3^{\frac{1}{2}}\frac{a^2}{R^2}\left[\tan^{-1}\frac{2(1-a/R)^{\frac{1}{3}}+1}{3^{\frac{1}{2}}}-\tan^{-1}\frac{1}{3^{\frac{1}{2}}}\right]\right\}. \quad (8)$$

Eq. (8) corresponds to the solutions of McCoy,[1] v. Schweidler[2] and Flamm[3] and is plotted on Figs. 6 and 7 for comparison with the exact result of Eq. (6). When $a=0$, Eq. (8) gives $\epsilon=0.150$, whereas the true value of ϵ is always lower; see Fig. 6.

Fig. 8 shows the ionization factor $\epsilon_a kR$ for all known alpha-particles. Three absorbers $a=0$, $a=0.5$ cm, $a=1.63$ cm of air at 0°C and 760 m Hg are considered. The factor $\epsilon_a kR$ is a direct measure of the ionization as a function of R above sources having the same N and μ. Such a case is presented when a single source contains several radioactive substances in equilibrium, e.g., an igneous rock source which contains all members of the U, Ac and Th series.

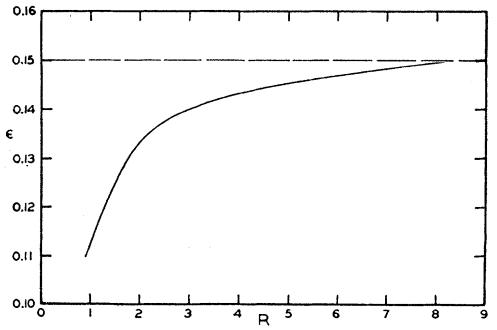

FIG. 6. The solid curve is the empirical value of ϵ, the coefficient of Eq. (7), as a function of the range, R, of the alpha-particle in air at 0°C and 760 mm Hg. The dotted line is the value of ϵ given by the approximate theory of Eq. (8), employing the two-thirds power rule of Eqs. (1) and (3).

IV. Stratification of Ionization above a Thick Plate

The total ionization to any height above a thick source may be derived from the results of Section III. The ionization chamber, of thickness a' is regarded as an additional absorber. The ionization measured in it is the ionization lost in an additional absorber of thickness a', or $q_a-q_{a+a'}$. The fraction of the total available ionization which is observed in the chamber is then $q_a/q-q_{a+a'}/q$. Numerical values, for alpha-particles of any range, R, may be read from Fig. 7. For the special case in which $a=0$, the fractional ionization absorbed in the chamber is $1-q_{a'}/q$. Ordinates corresponding to this case are shown at the right side of Fig. 7.

The exact nature of the variation of ionization with distance is important in measurements on very feeble sources, such as rocks, where the ionization chamber must be made as shallow as possible, so that its background ionization from cosmic and local radiation will be sufficiently low.

V. Ionization above Thin Sources

The ionization above a thick source may be thought of as composed of two parts: first, the ionization from a thin surface layer; second, the ionization from below this layer. The ionization from below equals that due to a thick source surmounted by the thin surface layer acting as an absorber. The equations are therefore the same as those of the preceding section. The total ionization from a thin layer of thickness a is $q-q_a$, hence the fractional ionization relative to that from a thick source is $1-q_a/q$; these values are shown as ordinates on the right side of Fig. 7.

VI. Counting Individual Alpha-Particles

In examining weak sources it is sometimes more convenient to count individual alpha-particles than to measure the ionization current produced by them. Several devices, aside from cloud chambers, are available for such measure-

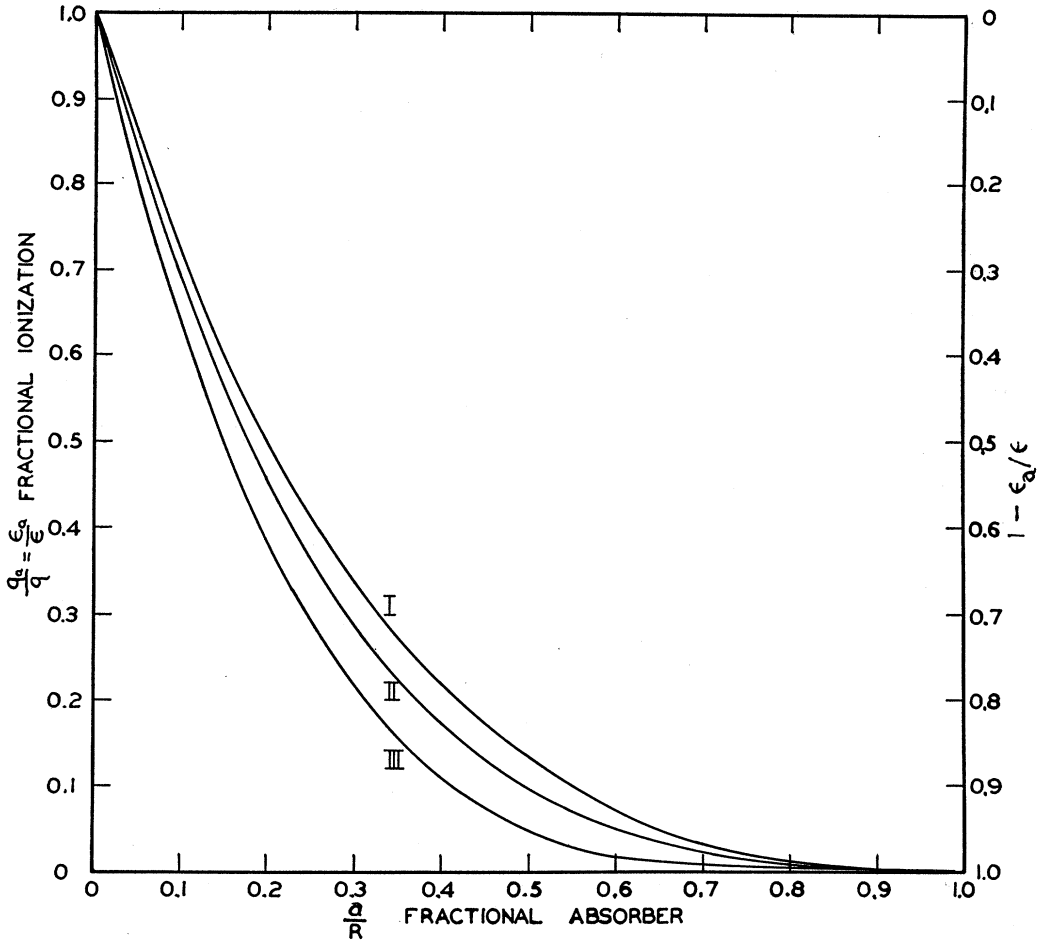

FIG. 7. Curves for absorption, stratification of ionization, and ionization from thin sources, for alpha-particles. Ordinates at the left, q_a/q or ϵ_a/ϵ, show the fraction of the maximum ionization which remains above the absorber; see Section III of the text. The ordinates at the right are $1-\epsilon_a/\epsilon$; see Sections IV and V of the text. Curve I is for long range alpha-particles; the computed values from the exact theory for 6.6 cm alpha-particles coincide with the values from the approximate theory of Eq. (8). Curve II is for the 2.56 cm alpha-particles from U I. Curve III is for 1.0 cm alpha-particles.

ments.[13] Where the alpha-particle pulse counter is an air-filled ionization chamber connected to a linear amplifier, it is possible to recognize a particle whose path in the ionization chamber is 0.2 cm or greater. If we designate this minimum track length for detection as ρ cm of air, then the following analysis applies.

In Fig. 5 let the source have a thickness μd and hence be equivalent in stopping power to d cm of air. The number of particles per cm^2 of surface which spend their range beyond r in the counting apparatus and hence emerge from the interface CC' with residual ranges $\rho \geq R-r$ is given by integrating Eq. (4) between the limits $x=0$ and $x=\mu d$, and making the substitution $r \equiv R-\rho$. This is:

$$n_a = (N\mu d/4)\cdot[2(R-\rho-a)-d]/(R-\rho), \quad (9)$$

which is the counting rate for thin films surmounted by absorbers.

For thick films, d has its maximum value which is $d=r-a=R-\rho-a$; substituting in Eq.

[13] Greinacher, Zeits. f. Physik **36**, 364 (1926); **44**, 319 (1927). Wynn-Williams and Ward, Proc. Roy. Soc. **A131**, 391 (1931). Curtiss, Bur. Standards J. Research **9**, 115 (1932). Bearden, Rev. Sci. Inst. **4**, 271 (1933). Hafstad, Phys. Rev. **44**, 201 (1933).

(9) we have the counting rate for thick films:

$$n_a=(N\mu/4)\cdot(R-\rho-a)^2/(R-\rho). \qquad (10)$$

As an example consider counting the 1.13 cm alpha-particles from samarium.[4, 5] If the emitter is a block of samarium sulfate, $Sm_2(SO_4)_3\cdot 8H_2O$, then the Bragg-Kleeman rule gives $\mu=3.49\times10^{-4}$. Having a density of 2.93 g per cm³, the material should emit[4] 90 alpha-particles per cm³ per sec. If the counting chamber is separated from the source by 1 mm of air, then $a=0.1$ cm, and if residual ranges of 2 mm or greater will operate the counter, then $\rho=0.2$ cm. Substituting in Eq. (10), we find 0.35 counts per cm² per min. In determining the effective area, the counting chamber's geometry must be considered.

VII. Corrections for Straggling

The use of the extrapolated ionization curve of Fig. 4 automatically corrects the ionization Eq. (6) for straggling.

The probability, P_l, that the range-element r, (measured from the origin of the track, in equivalent cm of air) will be lengthened or shortened by l cm is

$$P_l=(1/\rho_3 r\pi^{\frac{1}{2}})e^{-l^2/\beta_3^2 r^2}.$$

Eqs. (9) and (10), for counting individual particles, are corrected for straggling by integrating the above error function describing straggling over the appropriate solid angles. Since the error function is symmetrical, the gain due to straggling is only slightly less than the loss. Detailed treatment shows that the fractional loss, $\Delta n/n$, of countable particles is:

$$\Delta n/n=\tfrac{1}{2}(\rho_3)^2, \qquad (11)$$

where the fourth power of ρ_3 is neglected, and $\rho_3 r$ is the usual straggling or distribution coefficient. Briggs[14] has determined ρ_3 experimentally at various points along the range of Ra C′ alpha-particles, finding values between 0.0778 at $r=0.5$ cm and 0.0177 at 6.5 cm. The maximum loss in counting rate due to straggling is therefore only 0.3 percent. Strictly, the range employed in Eqs. (9) and (10) for counting alpha-particles is the most probable range, which, according to Kurie's[15] analysis of Briggs[14] data, is shorter than the usual extrapolated ionization range by 0.042 $(R-1.51)^{\frac{1}{2}}$ cm.

[14] Briggs, Proc. Roy. Soc **A114**, 313 (1927).
[15] Kurie, Phys. Rev. **41**, 701 (1932).

VIII. Total Ionization above Plates with Mixed Ranges

In considering the radiation from polished surfaces of ordinary rocks, we deal with the integrated effect of all the different alpha-particles of the U, Th and Ac series. If no absorber is used, $a=0$, $q_a\equiv q$, $\epsilon_a\equiv\epsilon$, and for the uranium series Eq. (7) becomes:

$$q^{U}=N^{U}\sum\epsilon kR\mu, \qquad (12)$$

where the summation extends over all the alpha-ray emitting elements in the uranium series, and is evaluated with the aid of Figs. 1 and 6. Similar expressions may be written for the thorium and actinium series.

For every element which has been proved to emit alpha-rays, Table I gives the extrapolated ionization range, $R_{15°}$, in air at 15°C, 760 mm; the

Table I. *Extrapolated ionization range, ionization, ϵ, and ionization factor for all known alpha-particles.*

Element	$R_{15°}$	R	$k\times10^5$	ϵ	$\epsilon kR\times10^5$	$\Sigma\epsilon kR$
U I	2.70	2.56	1.17	0.138	0.41	
U II	3.28	3.11	1.33	0.140	0.58	
Io	3.19	3.03	1.31	0.140	0.55	
Ra	3.39	3.21	1.36	0.141	0.62	corrected for C, C′, C″ branching
Rn	4.12	3.91	1.55	0.143	0.87	
Ra A	4.72	4.48	1.70	0.144	1.10	
Ra C	4.14	3.92	1.56	0.143	0.87	
Ra C′	6.97	6.60	2.20	0.148	2.15	
Ra F	3.92	3.72	1.50	0.142	0.79	
U series						7.07×10^5
Th	2.90	2.75	1.22	0.139	0.47	
Rd Th	4.02	3.81	1.53	0.143	0.83	
Th X	4.35	4.12	1.61	0.144	0.96	
Tn	5.06	4.80	1.78	0.145	1.24	
Th A	5.68	5.39	1.92	0.146	1.51	
Th C	4.79	4.54	1.71	0.144	1.12	
Th C′	8.62	8.17	2.54	0.150	3.11	
Th series						7.42×10^5
Ac U	3.2(?)	3.0	1.31	0.140	0.54	
Pa	3.67	3.48	1.43	0.142	0.71	
Rd Ac	4.68	4.43	1.69	0.144	1.08	
Ac X	4.37	4.14	1.62	0.143	0.96	
An	5.79	5.49	1.95	0.146	1.57	
Ac A	6.58	6.24	2.12	0.147	1.95	
Ac C	5.51	5.22	1.89	0.146	1.44	
Ac C′	6.5	6.2	2.10	0.147	1.92	
Ac series						8.25×10^5
Sm	1.13	1.06	0.56	0.114	0.068	

range, R, at 0°C, 760 mm; the total ionization, k, per alpha-particle; the coefficient ϵ of Eq. (7); and the ionization factor ϵkR. The last column gives $\sum \epsilon kR$ for the U, Th and Ac series, where the branching ratios of the C, C′ and C″ bodies have been taken into account in making the summation. The range of the actinouranium (Ac U) alpha-particle was estimated from the half-value period given by v. Grosse,[16] combined with the Geiger-Nuttall relation by using Geiger's values for the Ac series.[10]

The stopping power of rocks relative to air at 0°C and 760 mm depends on the composition of the rock, in accord with the Bragg-Kleeman rule. We can form an independent estimate of μ for rocks from measurements of the radius of the Ra C′ pleochroic halo ring, which has values between 28 and 34×10^{-4} cm in various minerals.[17] Taking 31×10^{-4} cm as an average value, we find $\mu=4.7\times10^{-4}$, and this is in fair agreement with the value computed from the chemical composition, using the Bragg-Kleeman rule.

If U is the concentration of uranium I in g per g of rock, and d the density of the rock, then since the decay constant[18] $\lambda_{U\,I}$ is 4.77×10^{-18} sec.$^{-1}$, and the atomic weight 238.14, we can express N^U, the number of uranium-I alpha-particles per cm^3 of rock per sec., as

$$N^U = \mathrm{U}\cdot d\cdot\frac{6.06\times10^{23}\times4.77\times10^{-18}}{238.14} = 1.22\times10^4\ \mathrm{U}\cdot d. \quad (13)$$

Similarly we find for N^{Th}, the number of thorium alpha-particles per cm^3 of rock per sec.,

$$N^{Th} = \mathrm{Th}\cdot d\cdot\frac{6.06\times10^{23}\times1.2\times10^{-18}}{232.12} = 0.31\times10^4\ \mathrm{Th}\cdot d, \quad (14)$$

where Th is the concentration of thorium in g per g of rock. For the actinium series, whose parent is Ac U, an isotope of U I, we take the activity ratio of v. Grosse;[16] thus 0.04 alpha-particles from Ac U accompany each alpha-particle from U I, hence:

$$N^{Ac} = 0.04\ N^U = 0.05\times10^4\ \mathrm{U}\cdot d. \quad (15)$$

Combining Eqs. (12) to (15) with the data of Table I, then taking $\mu=4.7\times10^{-4}$ we find

$$q^U = 8.62\times10^9\mu\mathrm{U}\cdot d = 4.06\times10^6\ \mathrm{U}\cdot d, \quad (16)$$
$$q^{Ac} = 0.43\times10^9\mu\mathrm{U}\cdot d = 0.20\times10^6\ \mathrm{U}\cdot d,$$
$$q^{Th} = 2.30\times10^9\mu\mathrm{Th}\cdot d = 1.08\times10^6\ \mathrm{Th}\cdot d.$$

Since ordinary granites have a uranium content of *ca.* 3×10^{-6} g U per g, a thorium content of *ca.* 6×10^{-6} g Th per g, and a density of *ca.* 2.7 g per cm^3, the total ionization is $\sum q = q^U+q^{Ac}+q^{Th} = 32.8+1.6+17.5 = 51.9$ ion pairs per cm^2 of rock surface per second. Where a shallow ionization chamber is employed, this alpha-ray ionization will more than double the background ionization from cosmic and local gamma-radiation, and is therefore within the range of modern apparatus. The saturation current is the order of 10^{-15} amp. per 100 cm^2 of rock.

The ranges given in Table I are those of Rutherford, Chadwick and Ellis.[19] Recent determinations by various workers, as summarized by Kurie and Knopf,[20] suggest no striking changes. The decay constant, 1.2×10^{-18} sec.$^{-1}$, for Th is that of the International Radium-Standards Commission.[21] If the higher value of 1.7×10^{-18} sec.$^{-1}$ found by Geiger and Rutherford[22] is taken, then the numerical constant of Eq. (14) *et seq.* would be correspondingly modified. The actinium series branching ratio is taken[16] as 0.04 in Eqs. (15) and (16). If the lower value of 0.03 as obtained by Hahn and Meitner,[23] who used tantalum for the separation of protactinium, is employed, then the numerical coefficient of Eq. (15) and of the actinium member of Eq. (16) would be reduced correspondingly.

[16] A. v. Grosse, Phys. Rev. **42**, 565 (1932).

[17] Holmes, Nat. Res. Council, Bull. **80**, 162 (1931).

[18] Kovarik and Adams, Phys. Rev. **40**, 718 (1932) give $\lambda_{U\,I}=4.865\times10^{-18}$ sec.$^{-1}$. When corrected for AcU, this value becomes 4.77×10^{-18} sec.$^{-1}$.

[19] Rutherford, Chadwick and Ellis, *Radiations from Radioactive Substances* pp. 24–27 (1930).

[20] Kurie and Knopf, Phys. Rev. **43**, 311 (1933).

[21] Rev. Mod. Phys. **3**, 427 (1931).

[22] Geiger and Rutherford, Phil. Mag. **20**, 691 (1910).

[23] Hahn and Meitner, Phys. Zeits. **20**, 529 (1919); Zeits. f. Physik **8**, 202 (1922).

IX. Total Ionization above Plates with Mixed Ranges and Surmounted by Absorbers

In measuring the ionization above say 100 cm² of polished rock surface, the specimen cannot be placed inside the ionization chamber, both because of its size and because of the distortion it would produce in the electrostatic ion-collecting field with a resultant influence on the relative saturation of the ion current. If the rock surface is brought close to a thin aluminum foil window in the ionization chamber, and if the total stopping power of the window and air between the rock surface and the inside of the ionization chamber is equivalent to a cm of air at 0°C and 760 mm, then a/R can be computed for each alpha-particle range involved. Fig. 7 then gives ϵ_a/ϵ, and combined with the values of ϵkR from Table I we can easily evaluate the total ionization, q_a, per cm² per sec. for each radiaoctive element, using Eq. (7). Fig. 8 shows the value of the ionization factor $\epsilon_a kR$ for all values of R and for $a=0$ (no absorber); $a=0.5$ cm air-equivalent at 0°C, 760 mm; and $a=1.63$ cm air-equivalent at 0°C, 760 mm. For the present case, with absorption, Eq. (12) becomes

$$q_a{}^{U} = N^{U}\Sigma\epsilon_a kR\mu \qquad (17)$$

with similar equations for the thorium and actinium series. Tabulating $\epsilon_a kR$ from Fig. 8, and summing over each of the radioactive series, we obtain the values shown in Table II for the

Table II. *Series ionization factors and relative ionization for U, Th, Ac series and Sm, with and without absorbers.*

	$a=0$		$a=0.5$ cm air 0°C, 760 mm		$a=1.63$ cm air 0°C, 760 mm	
	$10^{-5}\Sigma\epsilon kR$	q/q	$10^{-5}\Sigma\epsilon_a kR$	q_a/q	$10^{-5}\Sigma\epsilon_a kR$	q_a/q
U series	7.07	1.00	4.58	0.65	1.60	0.23
Th series	7.42	1.00	5.23	0.70	2.27	0.31
Ac series	8.25	1.00	5.72	0.69	2.30	0.28
Sm	0.068	1.00	0.0041	0.06	0	0

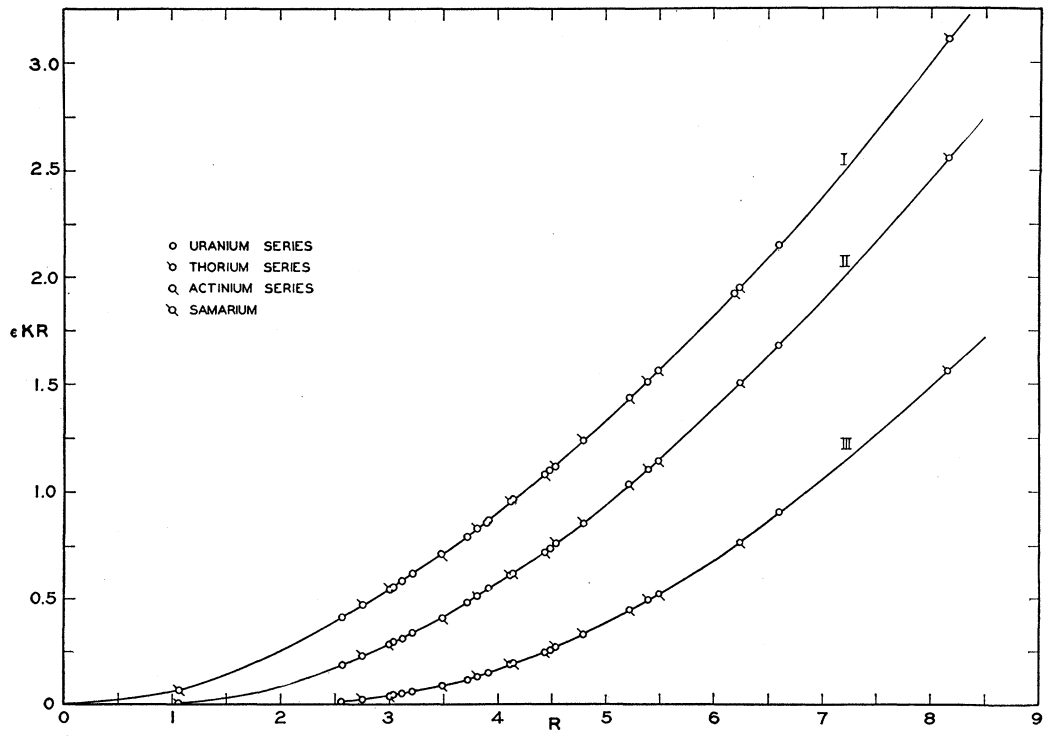

Fig. 8. The ionization factor, $\epsilon_a kR \times 10^{-5}$, for all known natural alpha-particles; see Eq. (7). R is the range of the alpha-particle in cm of air at 0°C and 760 mm Hg. Curve I shows ϵkR (no absorber). Curve II shows $\epsilon_a kR$ with an absorber of 0.5 cm air-equivalent at 0°C and 760 mm Hg. Curve III shows $\epsilon_a kR$ when $a=1.63$ cm air-equivalent. Intermediate values for other absorbers may be obtained by interpolation or by computation from Figs. 1, 6 and 7.

series ionization factor $\sum \epsilon_a k R$, and for the fraction, q_a/q, of the total ionization from the radioactive surface which is able to penetrate the absorber and appear in the ionization chamber. It will be noted that, when radioactive equilibrium exists, the uranium series is more strongly absorbed by a given absorber than is the actinium series, and that the thorium series is absorbed the least of the three. This is due, of course, to the longer ranges of many of the thorium series alpha-particles. The difference in absorbability between the U, Th and Ac series is, however, not great enough to afford a means of separating these effects and determining, from absorption measurements, both the uranium and thorium content of feebly radioactive materials.